Synthesis and Photoluminescent Properties of $Sr_3Gd_2(BO_3)_4$: Tb^{3+} Phosphors

Sheetal[1], Ritu Langyan[2], Sonika[1,*], S.P. Khatkar[1], Rajesh Kumar[3]

[1]Department of Chemistry, Maharshi Dayanand University, Rohtak - 124001, India
[2]Department of Chemistry, Kurukshetra University, Kurukshetra – 136119, India
[3]Department of Applied Sciences, UIET, Maharshi Dayanand University, Rohtak - 124001, India

ABSTRACT

Tb^{3+}-activated $Sr_3Gd_2(BO_3)_4$ nanophosphors have been synthesized by combustion route using glycine as fuel. Morphology and luminescent properties of $Sr_3Gd_2(BO_3)_4$:Tb^{3+} nanoparticles were characterized by scanning electron microscopy, fluorescence spectrometry, and x-ray diffraction. The X-ray diffraction patterns (XRD) were used to investigate phase and average grain size is less than 1μm in temperature range 700°C to 1000°C. The emission spectra indicated the excellent green photoluminescent properties of $Sr_3Gd_2(BO_3)_4$:Tb^{3+} phosphors due to characteristics transition of Tb^{3+} ions from $^5D_4 \rightarrow {}^7F_5$ at 545 nm. The dependence of the luminescence intensity on Tb^{3+} ions concentrations and effect of heat treatment have also been discussed.

Keywords: *$Sr_3Gd_2(BO_3)_4$:Tb^{3+}, Nanophosphor, Green luminescence, Crystal structure.*

*Corresponding Author: Tel: +91 8198918182

E-mail address: sssonicasingh31@gmail.com (Sonika)

1. INTRODUCTION

Modern optoelectronic devices require phosphor materials to convert UV or near UV-blue radiation into visible light. Different kinds of inorganic phosphors based on lanthanides are used for this purpose, such as aluminates, phosphates, oxides, silicates and borates [1,2]. Rare earth orthoborate phosphors are quite promising and recently studied class of phosphors [3]. Borate-based phosphor materials may be applied in different devices like luminescent tubes and plasma display panels as well as light emitting diodes [4-6]. Eu^{3+} doped yttrium-gadolinium borate $(Y_xGd_{1-x})BO_3$ and yttrium borate YBO_3 and are known as commercial red phosphors applicable in plasma display panels (PDP) [1]. Tb^{3+} ions have been expected to be a promising species for providing optical devices in blue and green color regions and many investigations have been conducted in various compounds [7,8]. In the past, the luminescence properties of Tb^{3+} in different host matrix were also extensively studied [9,10]. With Tb^{3+} activation, the emission is from $^5D_3$ and $^5D_4$ states to ^7F states. The main green emission is from the $^5D_4$ state at 545 nm. Mixed Sr-La, Sr-Y and Sr-Gd borates have been successfully synthesized by solid state method [11,12]. Wet chemical methods are known to be better than solid-state reaction methods in intimate mixing of reactants, high product purity, fine particle size and low processing temperature [13]. Combustion can produce a homogenous product in a short duration of time without the use of expensive high-temperature furnaces and enhances the distribution of Tb^{3+} in the $Sr_3Gd_2(BO_3)_4$ host lattice.

2. EXPERIMENTAL

2.1. *Powder Synthesis*

$Sr_3Gd_{2(1-x)}(BO_3)_4:2xTb^{3+}$ was synthesized by combustion method using high purity starting reagents $Sr(NO_3)_2$, $Gd(NO_3)_3.6H_2O$, H_3BO_3, $Tb(NO_3)_3.6H_2O$ and glycine. According to nominal composition of $Sr_3Gd_{2(1-x)}(BO_3)_4:2xTb^{3+}$ (x=0.01, 0.03, 0.05, 0.07 and 0.09), a stoichiometric amount of metal nitrates and boric acid were dissolved in minimum quantity of deionized water in 200 mL capacity pyrex beaker. Then glycine was added in this solution with molar ratio of glycine to oxidizer based on total oxidizing and reducing valencies of oxidizer and fuel (glycine) according to concept used in propellant chemistry. Finally the beaker containing the solution was placed into a preheated furnace maintained at 550°C. The material undergoes rapid dehydration and foaming followed by decomposition, generating combustible gases. The powders obtained were calcined at different temperatures from 700°C to 1000°C for 3 h to increase the brightness.

2.2. Powder Characterization Techniques

Crystal phase of $Sr_3Gd_2(BO_3)_4:Tb^{3+}$ powders were characterized by Rigaku Ultima-IV X-ray powder diffractometer with CuKα radiation to record the patterns in 2θ range of 10°-70°. Surface morphology was evaluated using Jeol JSM-6510 scanning electron microscope. Excitation and emission spectra of powders in the ultraviolet-visible region were obtained at room temperature using Hitachi F-7000 fluorescence spectrophotometer with Xe- lamp as the excitation source. All the properties were investigated at room temperature.

3. RESULTS AND DISCUSSION

3.1. X-ray Diffraction Studies

The XRD patterns of $Sr_3Gd_{1.86}Tb_{0.14}(BO_3)_4$ powders, as-prepared and calcined at different temperatures 700°C, 900°C and 1000°C for 3h are shown in fig.1. XRD patterns of the as-prepared samples at 550°C show many additional peaks corresponding to those of unreacted $Sr(NO_3)_2$ phase (JCPDS card no. 04-0310) and $Gd(NO_3)_3$ phase (JCPDS card no. 31-0529) respectively and no $Sr_3Gd_2(BO_3)_4$ phase formation was observed. At further higher temperature of 700°C, the peaks characteristic due to $Sr_3Gd_2(BO_3)_4$ phase appeared, while the peaks due to strontium nitrate and gadolinium nitrate disappeared. At this temperature (700°C) the characteristic peak intensity at 2θ = 28.657 was weak, but on further heating the sample at 900°C the enhancement of peak intensity is noticed. At 1000°C, a pure orthorhombic $Sr_3Gd_2(BO_3)_4$ phase was obtained which matched well with literature data [14].

The size of the crystallites can be estimated with the help of Scherrer equation, $D = 0.94\lambda/\beta\cos\theta$, where D is the average crystallite size, λ is X-ray wavelength (0.15418 nm), θ is the diffraction angles and β is full-width at half-maximum (FWHM, in radian) of an observed peak, respectively [15]. The calculated average crystallite size (D) of $Sr_3Gd_2(BO_3)_4:Tb^{3+}$ phosphor particles is found to be 21 nm at calcination temperature 700°C, 41 nm at calcination temperature 900°C and 69 nm at calcination temperatures of 1000°C. Hence, it can be concluded from the calculated results that with the increase of calcination temperature the crystallite size also becomes larger.

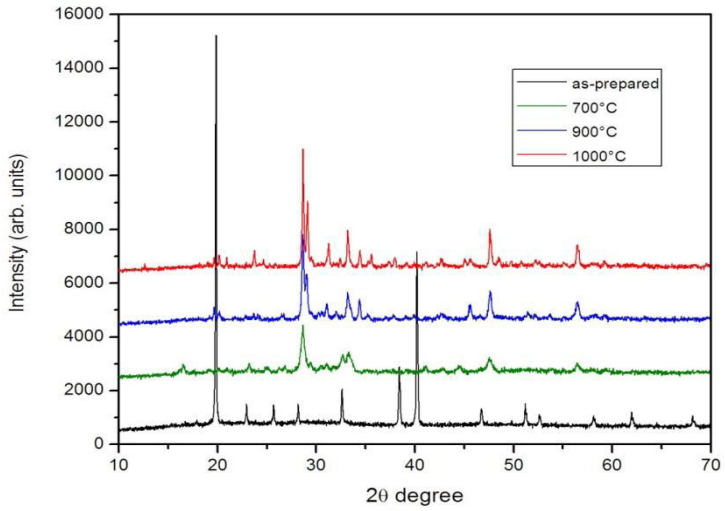

Fig.1. XRD patterns of $Sr_3Gd_{1.86}Tb_{0.14}(BO_3)_4$ powders calcined at various temperatures.

3.2. Morphological Characteristics

The surface morphological features of the powder phosphor were studied by scanning electron microscope (SEM). SEM images of $Sr_3Gd_{1.86}Tb_{0.14}(BO_3)_4$ phosphors, as-synthesized and calcined at 700°C, 900°C and 1000°C are displayed in fig. 2(a-d). The SEM image in fig. 2(a) indicates that the as-prepared sample primarily consists of lots of irregular shaped particles. The powders possess highly agglomerated crystallites. With an increase of temperature, particle size increased and agglomeration decreased. At 1000°C, smooth spherical particles are obtained. The micrograph indicates presence of grains of ~1μm in size.

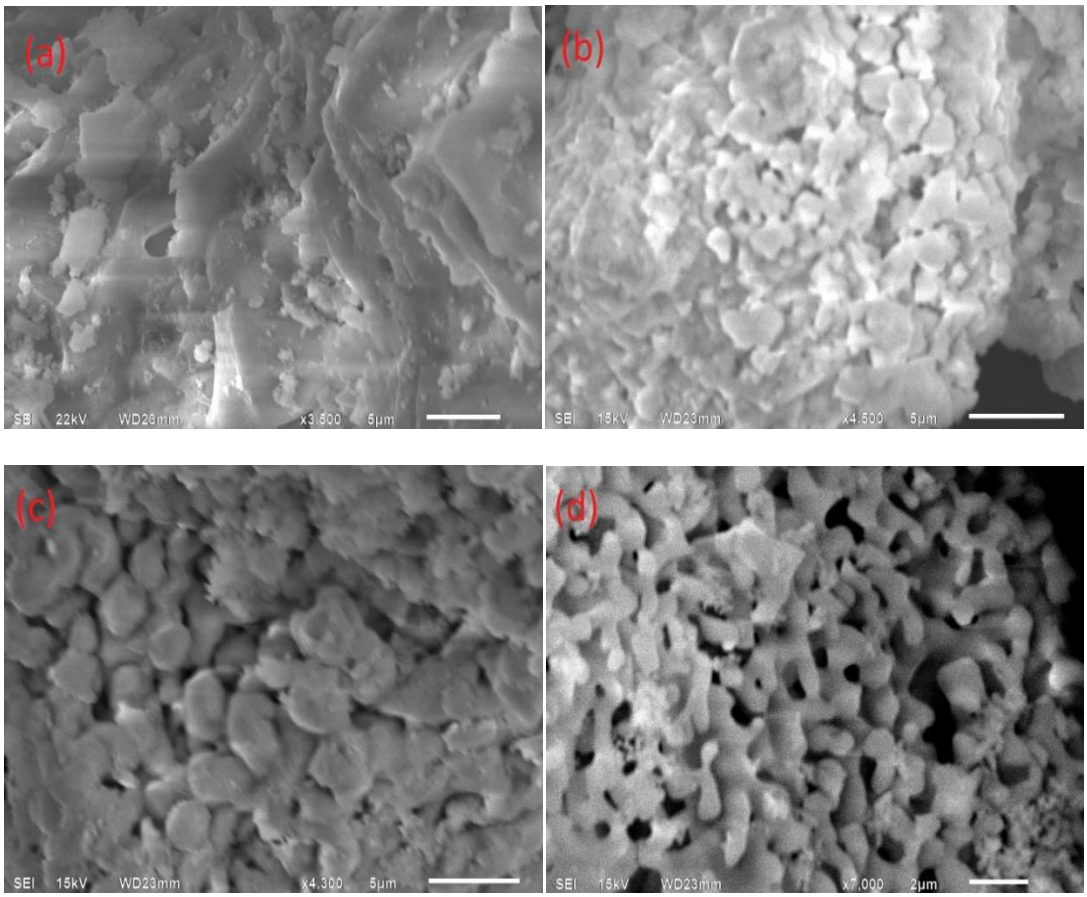

Fig.2. SEM micrographs of $Sr_3Gd_{1.86}Tb_{0.14}(BO_3)_4$ (a) as-synthesized; calcined at (b) 700°C (c) 900°C and (d) 1000°C temperatures.

3.3. Luminescent Properties

The photoluminescence excitation spectrum of $Sr_3Gd_{1.86}Tb_{0.14}(BO_3)_4$ calcined at 1000°C, at an emission wavelength of 545 nm ($^5D_4 \rightarrow {}^7F_5$ transition) is shown in fig. 3. Excitation spectrum consists of a broad intense band in the range from 200 nm to 280 nm with a maximum at 244 nm. The high intensity band at 244 nm is assigned to spin-allowed $4f^8–4f^75d^1$ transitions of Tb^{3+} ions in the $Sr_3Gd_2(BO_3)_4$ host lattice. The longer wavelength region of the spectrum beyond 330 nm comprises of some sharp peaks. These sharp peaks in the longer wavelength region are assigned to Tb^{3+} intra-4*f* transitions ($4f^8–4f^8$) from the ground state to higher energy levels. The dominant excitation peaks at 352 nm, 377 nm and 486 nm can be attributed to $^7F_6$-$^5D_2$, $^7F_6$-$^5D_3$ and $^7F_6$-$^5D_4$ transitions of Tb^{3+} respectively [16,17]. The peak observed at 280 nm and 313 nm due to $^8S_{7/2} \rightarrow {}^6I_J$ and $^8S_{7/2} \rightarrow {}^6P_J$ transition of Gd^{3+} respectively.

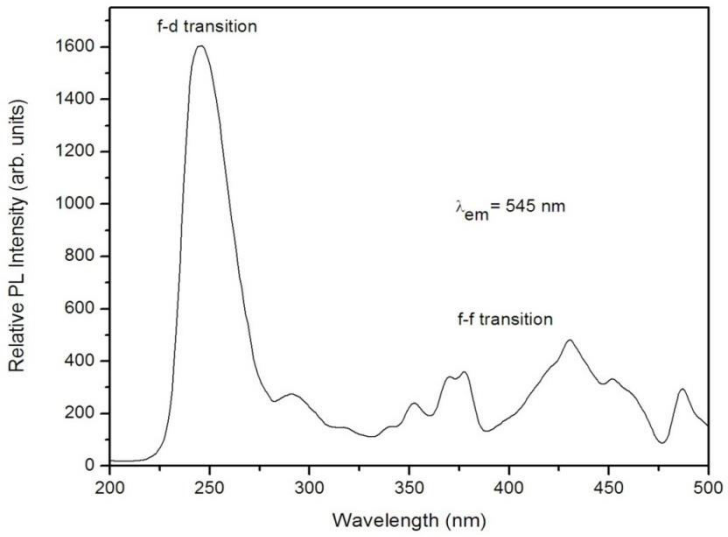

Fig.3. Excitation spectrum of $Sr_3Gd_{1.86}Tb_{0.14}(BO_3)_4$ sample calcined at 1000°C, λ_{em} = 545 nm.

The emission spectra of $Sr_3Gd_2(BO_3)_4$:Tb^{3+} under excitation wavelength of 244 nm are shown in fig. 4. The spectra comprises of stronger peaks due to Tb^{3+} transitions $^5D_4 \rightarrow {}^7F_5$, $^5D_4 \rightarrow {}^7F_4$ and $^5D_4 \rightarrow {}^7F_6$ at emission wavelengths 545 nm, 584 nm and 622 nm respectively [18,19]. The magnetic dipole transition $^5D_4 \rightarrow {}^7F_5$ (545 nm) is dominant resulting in green emission of the phosphor. In particular fig. 4(a) shows the relative photoluminescent intensity of $Sr_3Gd_{1.86}Tb_{0.14}(BO_3)_4$ as a function of temperature at λ_{ex}=244 nm. The photoluminescence spectra of phosphors were found to increase in intensity with calcination temperature up to 1000°C. The possible reason for the results are, firstly the good crystalline structure on calcination increases oscillator strength for optical transitions; secondly, improvement in crystalline size results in less light scattering at the surfaces and interfaces leading to strong PL; and the third, a larger amount of rare earth ions are embedded into the matrix with calcination [20]. The luminescence intensitie of the phosphors is dependent on the dopant concentration. Fig. 4(b) displays dependence of PL intensity of $Sr_3Gd_2(BO_3)_4$:Tb^{3+} on the concentration of dopant Tb^{3+}. It is quite clear that PL intensity of $Sr_3Gd_{2(1-x)}Tb_{2x}(BO_3)_4$ (x=0.01-0.09) increases with increasing Tb^{3+} concentration, reaching a maximum value at x=0.07 and thereafter decreases with further increase in Tb^{3+} concentration due to mutual Tb^{3+}-Tb^{3+} interactions.

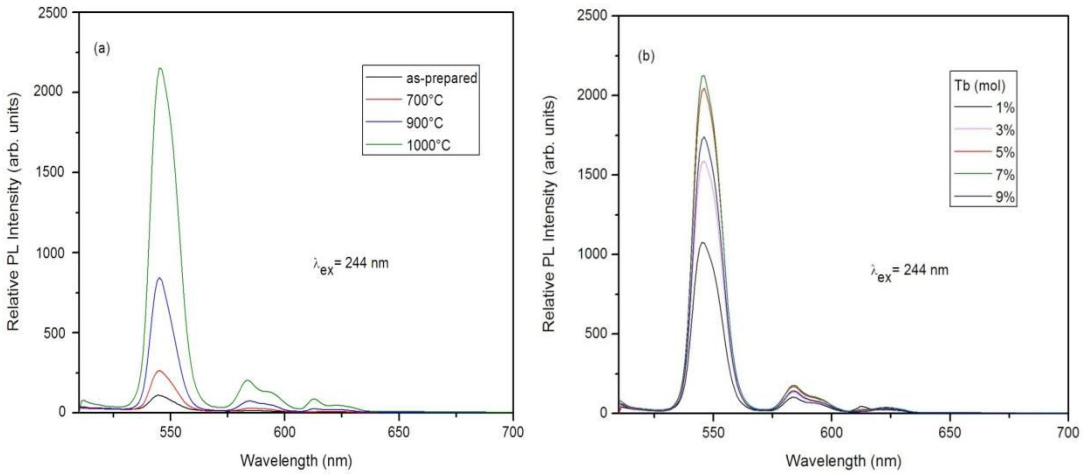

Fig.4. (a) Emission spectra of $Sr_3Gd_{1.86}Tb_{0.14}(BO_3)_4$ showing relative PL intensity as a function of temperature and (b) Emission spectra of $Sr_3Gd_{2(1-x)}(BO_3)_4$:2xTb^{3+} (x=0.01, 0.03, 0.05, 0.07 and 0.09) showing variation of emission intensity as a function of Tb^{3+} concentrations, λ_{ex}=244 nm.

4. CONCLUSION

$Sr_3Gd_2(BO_3)_4$:Tb^{3+} has been synthesized at 550°C by combustion method using glycine as an organic fuel. The solid obtained was again calcined at 700°C to 1000°C for 3 h to increase the brightness. XRD pattern showed that intensities and positions of diffraction peaks of $Sr_3Gd_2(BO_3)_4$:Tb^{3+} samples calcined to 1000ºC corresponds to that of pure orthorhombic structure $Sr_3Gd_2(BO_3)_4$ phase with Pc21n space group. The SEM image indicates that the as-prepared sample primarily consists of lots of irregular shaped particles. The powders possess highly agglomerated crystallites. With an increase of temperature, particle size increased and agglomeration decreased. The average grain size is less than 1μm in temperature range 700°C to 1000°C. The luminescence intensity was maximum with 7 mol% of Tb^{3+} in the host lattice. The main emission peak located at 545 nm corresponds to magnetic dipole transition $^5D_4 \rightarrow {}^7F_5$ of Tb^{3+} under excitation wavelength of 244 nm.

REFERENCES

1. C.H. Kim, I.E. Kwon, C.H. Park, Y.J. Hwang, H.S. Bae, B.Y. Yu, C.H. Pyun, G.Y. Hong, *J. Alloys Compd*., 311 (2000) 33.
2. S. Ye, F. Xiao, Y.X. Pan, Y. Ma, Q.Y. Zhang, *Mater. Sci. Eng. R*, 71 (2010) 1.
3. A.A. Shyichuk, S. Lis, *J. Rare Earths,* 29 (2011) 1161.
4. S. Ekambaram, K.C. Patil, M. Maaz, *J. Alloys Compd.,* 393 (2005) 81.
5. Z. Li, J. Zeng, C. Chen, Y. Li, *J. Cryst. Growth*, 286 (2006) 487.
6. A. Lakshmanan, R.S. Bhaskar, P.C. Thomas, R.S. Kumar, V.S. Kumar, M.T. Jose, *Mater. Lett*., 64 (2010) 1809.
7. H.J. Lozykowski, W.M. Jadwisienczak, I. Brown, *Appl. Phys. Lett.,* 76 (2000) 861.
8. W. Chen, R. Sammynaiken, Y. Huang. *J. Appl. Phys.,* 88 (2000) 1424.
9. R.P. Rao, W.W. Duley, *J. Mater. Sci.,* 27 (1992) 5883.
10. W.F. Vander Weg, T.J.A. Popma, A.T. Vink, *J. Appl. Phys.,* 57 (1985) 5450.

11. R. Zhang, X. Wang, *J. Alloys Compd.*, 509 (2011) 1197.
12. T.W. Kuo, T.M. Chen, *J. Lumin.*, 130 (2010) 483.
13. R.C. Anderson, W.J. Thomson, *Adv. Ceram.,* 27 (1994) 13.
14. Z. Rui, W. Xiang, *J. Alloys Compd.,* 509 (2011) 1197.
15. X.Q. Zeng, G.Y. Hong, H.P. You, X.Y. Wu, Chin. *J. Lumin.,* 22 (2001) 58.
16. Y. Yang, A. Bao, H. Lai, Y. Tao, H. Yang, *J. Phys. Chem. Solids,* 70 (2009) 1317.
17. G. Li, Y. Lai, W. Bao, L. Li, M. Li, S. Gan, T. Long, L. Zou, *Powder Technol.,* 214 (2011) 211.
18. Z.J. Zhang, J.L. Yuan, H.H. Chen, X.X. Yang, J.T. Zhao, G.B. Zhang, C.S. Shi, *Solid State Sci.,* 11 (2009) 549.
19. U. Rambabu, D.P. Amalnerkar , B.B. Kale, S. Buddhudu, *Mater. Chem. Phys.,* 70 (2001) 1.
20. Y. Zhang, Z. Lin, L. Zhang, G. Wang, *Opt. Mater.,* 29 (2007) 543.